



Cite this: *J. Mater. Chem. B*, 2015, **3**, 5080

Tailored polymeric membranes for Mycobacterium smegmatis porin A (MspA) based biosensors†

Danielle Morton,^a Shahab Mortezaei,^a Sukru Yemenicioglu,^a Michael J. Isaacman,^a Ian C. Nova,^b Jens H. Gundlach^b and Luke Theogarajan^{*a}

Nanopores based on protein channels inserted into lipid membranes have paved the way towards a wide-range of inexpensive biosensors, especially for DNA sequencing. A key obstacle in using these biological ion channels as nanodevices is the poor stability of lipid bilayer membranes. Amphiphilic block copolymer membranes have emerged as a robust alternative to lipid membranes. While previous efforts have shown feasibility, we demonstrate for the first time the effect of polymer composition on MspA protein functionality. We show that membrane–protein interaction depends on the hydrophobic–hydrophilic ratio (f -ratio) of the block copolymer. These effects are particularly pronounced in asymmetric protein pores like MspA compared to the cylindrical α -hemolysin pore. A key effect of membrane–protein interaction is the increased $1/f^2$ noise. After first showing increases in $1/f^2$ behaviour arise from increased substate activity, the noise power spectral density $S(f)$ was used as a qualitative tool for understanding protein–membrane interactions in polymer membranes. Polymer compositions with f -ratios close to lipid membranes caused noise behaviour not observed in lipid membranes. However, by modifying the f -ratio using a modular synthetic approach, we were able to design a block copolymer exhibiting noise properties similar to a lipid membrane, albeit with better stability. Thus, by careful optimization, block copolymer membranes can emerge as a robust alternative for protein-pore based nano-biosensors.

Received 26th February 2015,
Accepted 5th May 2015

DOI: 10.1039/c5tb00383k

www.rsc.org/MaterialsB

Introduction

Ion channels are intriguing nanoscale devices useful for constructing a wide-range of biosensors. A key application is rapid DNA sequencing using nanopores. Blockage of ionic current flowing through the protein pore by DNA in a base specific manner is the key to rapid electronic DNA sequencing.¹ Separation between bases is approximately 0.3 nm precluding the use of long cylindrically shaped channels such as α -hemolysin. Mycobacterium smegmatis porin A (MspA) has recently emerged as the protein of choice for sequencing applications due to its cone-like shape terminating in a single narrow (1.2 nm) opening and about 0.6 nm long constriction, enabling single base resolution.^{2,3}

Functional ion channels, such as MspA, require reconstitution in lipid membranes, which have limited stability. Lipid constituents are labile, expensive, and cannot tolerate harsh environments.⁴

Additionally, lipid membranes have characteristically short and highly variable lifetimes,⁵ ranging from a few minutes to a day. Block copolymer membranes based on either di- or tri-blocks are robust counterparts exhibiting extended lifetimes.⁶ More importantly, polymer membranes can be tuned by controlling hydrophobic/hydrophilic length and polymer composition.⁷

Amongst the myriad of choices of hydrophobic and hydrophilic blocks comprising the amphiphilic di- or tri-block copolymer, the polysiloxane hydrophobic core, due to its low glass-transition temperature, is unrivalled in its ability to support protein functionality.^{8,9} Therefore, we chose a tri-block copolymer of poly(methyloxazoline)–poly(dimethylsiloxane)–poly(methyloxazoline) (PMOXA–PDMS–PMOXA) as a lipid mimic. These ABA copolymers showed dramatically increased membrane stability compared to traditional lipids.⁸ Utilizing a unique modular synthesis, a systematic study of block copolymer composition on protein function is enabled, allowing for optimization of the block copolymer.⁷

We have previously shown the core principles of DNA sequencing using protein nanopores by utilizing a protein motor complex, a phi29 DNA polymerase, and the MspA pore.¹⁰ However, realizing a point-of-care device requires a more robust platform. Here we demonstrate for the first time, a single MspA insertion into a polymer membrane (Fig. 1a) and compared the results to an

^a Department of Electrical and Computer Engineering, University of California, Santa Barbara, CA, 93106, USA. E-mail: ltheogar@ece.ucsb.edu

^b Department of Physics, University of Washington, Seattle, WA 98195, USA

† Electronic supplementary information (ESI) available: Detailed protocols for membrane formation and data acquisition; membrane breakdown studies; polymer characterization; MspA pore I - V curves; noise dependence on bias spectra; additional current traces. See DOI: 10.1039/c5tb00383k

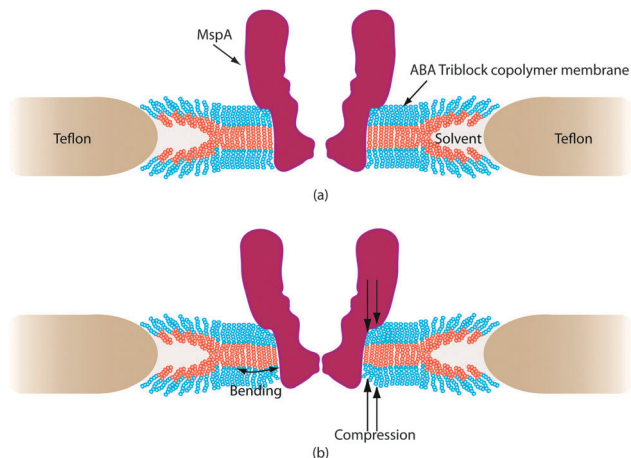


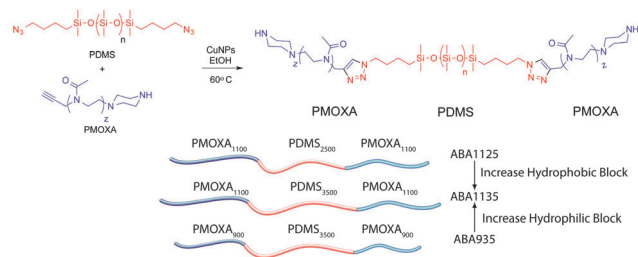
Fig. 1 Cartoon representation (not to scale) of MspA inserted into a polymer membrane. (a) MspA inserted into an optimized polymer membrane experiences very little stress due to membrane–protein interaction. (b) MspA inserted into an unoptimized polymer membrane experiences considerable conformational changes due to the polymer segments undergoing compressive and bending membrane interaction.

α -hemolysin insertion into a polymer membrane with the same composition. More importantly, we investigated the source of the differences in protein functionality (MspA versus α -hemolysin) by modulating the hydrophobic–hydrophilic ratio (f -ratio) of the block copolymer. As the polymer composition of the membrane was varied, noticeable differences in the noise spectral density became apparent. Using an analysis technique developed by Bezrukov and Winterhalter *et al.*,¹¹ the source of these changes were identified as arising from increased substate activity likely due to membrane–protein interaction (such as bending or compression of the membrane, Fig. 1b). Having established noise spectral density as an effective tool for evaluating membrane–protein interaction, we studied the behaviour of MspA in three polymer compositions of different f -ratios. Subsequent rms current and spectral analysis of open channel ion currents revealed $1/f^\alpha$ characteristics not observed in MspA prior to this work, elucidating the importance of membrane–protein interaction in the design of robust biosensors.

Experimental procedures

Polymer synthesis

ABA triblock copolymers were prepared in a manner previously described by the group.⁷ Briefly, poly(methyloxazoline) (PMOXA) was synthesized using cationic ring opening polymerization and terminated using a BOC-protected piperazine, followed by an acid-catalyzed BOC deprotection. Poly(dimethylsiloxane) was synthesized using an acid catalyzed cationic ring-opening polymerization using tosylate end-blockers followed by nucleophilic substitution of the tosylate to a diazide. Copper catalyzed alkyne azide cycloaddition was used to connect the blocks *via* triazole heterocycles (Scheme 1). ¹H-NMR (NMR) spectra were recorded on a Bruker Avance DMX500MHz SB NMR Spectrometer by dissolving polymers in deuterated chloroform (CDCl₃). Gel permeation



Scheme 1 Azide–alkyne click reaction used to form ABA triblock co-polymers of PMOXA–PDMS–PMOXA.

chromatography (GPC) studies were performed using a Waters 2695 Separation Module equipped with a 2414 Refractive Index Detector and 2996 Photodiode Array Detector. When forming solutions of polymer in *n*-decane–CHCl₃ mixtures the chloroform was always added first to completely dissolve the polymer. Polymers are named according to approximate block molecular weights (PMOXA_{xa}–PDMS_{xb}–PMOXA_{xa}) where xa and xb are in g mol⁻¹. Polymers abbreviated as PMOXA₁₁₀₀–PDMS₃₅₀₀–PMOXA₁₁₀₀ (ABA1135), PMOXA₉₀₀–PDMS₃₅₀₀–PMOXA₉₀₀ (ABA935), and PMOXA₁₁₀₀–PDMS₂₅₀₀–PMOXA₁₁₀₀ (ABA1125).

Membrane formation solutions

Lipid painting solutions of diphytanol phosphatidylcholine DPhPC (Avanti Polar Lipids, AL) were made by dissolving 1.5 mg of lipid in 75 μ L *n*-decane and 25 μ L heptanol. ABA copolymer prepaint solutions were made by dissolving 1.5 mg of ABA in 100 μ L of chloroform (CHCl₃). The ABA membrane forming solutions were made by dissolving 1.5 mg of ABA in 70 μ L *n*-decane and 30 μ L of chloroform (CHCl₃). A 1 M KCl, 10 mM HEPES–KOH solution buffered at pH 7 was added to the *cis* and *trans* chamber of the setup.

Membrane stability

Membranes were subsequently formed using painting techniques at 1.5% w/v polymer concentration in a mixture of *n*-decane and chloroform. Both planar free-standing ABA copolymer membranes and diphytanoylphosphatidylcholine (DPhPC) lipid membranes were formed in a 50 micron Teflon aperture ($\pm 20\%$) (Eastern Scientific, LLC) by adapting a standard lipid membrane painting procedure.¹² Current-clamp experiments showed the increased stability of polymer membranes with minimum breakdown voltages of 900 mV, nearly double the ~ 500 mV breakdown voltage for lipids¹³ (see ESI[†]). Bilayer formation was observed through video microscopy (4 \times magnification) while simultaneously monitoring the ion current and performing capacitance measurements.

Protein incorporation

After characterizing membrane stability, protein incorporation experiments were performed in both DPhPC membranes and three ABA copolymer membranes. Once the thinned portion of the membrane was visible, 1 μ L of 1 μ g mL⁻¹ M2-MspA in 0.1% OPOE was added to the 1 mL chamber and stirred gently MspA mutant porin M2-MspA was selectively prepared and extracted

from *M. smegmatis*.³ Once single protein insertion was verified *via* discrete current jumps corresponding to the known conductance levels of M2-MspA (~ 1.6 nS), its behaviour was observed and recorded for five minutes under a bias voltage of 60 mV to prevent M2-MspA from gating.² Protein insertion was first verified in a DPhPC membrane and served as a control. Single M2-MspA protein insertion experiments were then performed (8–10 single insertion experiments for each polymer) for the three different ABA polymer membranes.

Data acquisition

Conductance measurements were taken using an Eastern Scientific Picoamp-300B with picoamp resolution modified to apply voltages up to 2 V. Data was acquired using a NI PCI-6024E Card with NI LabView Software at a rate of 10 kHz with a 2nd-order 1 kHz Bessel filter applied from the Picoamp-300B. Subsequent data processing was performed in Mathworks MATLAB software.

Results and discussion

Although PMOXA-PDMS-PMOXA triblock copolymers have emerged as an alternative biomimetic membrane for protein incorporation, such as OmpF, α -hemolysin and alamethicin,^{8,9,14} the membrane-protein interaction reduces the conductance by 10% compared to the conductance in the DPhPC lipid membrane.¹⁴ Detailed molecular simulations, supported by experimental results, reveal notable differences in how lipid and polymer membranes stabilize embedded proteins.¹⁵ Polymer membranes, unlike lipids, are relatively compressible and thus more tolerant to hydrophobic mismatch. Simulations have shown a relatively large (22%) hydrophobic mismatch between the polymer and protein can be accommodated. This increased flexibility comes at the cost of the polymer blocks, near the protein, becoming increasingly strained.¹⁶ Experimentally, this interaction results in a ‘noisier’ channel conductance. So while conductance is a good measure of protein functionality, it is not sufficient characterization for their use in biosensors. Since conductance of the pore is an average value it does not reflect the dynamic performance of the pore. Averaging effectively serves as a low pass filter with a very low cut-off frequency and reduces both the noise and the bandwidth of the observed signal. For many biosensing applications, especially DNA sequencing, bandwidth upwards of 1 kHz is necessary and in these cases the noise properties set the limit of detection. Thus characterizing and reducing the noise present in the system is crucial for optimal performance.

MspA versus α -hemolysin

Our approach was to first study the behaviour of MspA in ABA block copolymers (PMOXA₁₁₀₀-PDMS₂₅₀₀-PMOXA₁₁₀₀) (ABA1125, Scheme 1) in which insertion of proteins, such as α -hemolysin had been shown.¹⁴ Qualitatively, the differences in noise in the time trace between the two proteins in the same polymer membrane appeared significant (see ESI,† Fig. S6).

Noise is best studied in the frequency domain and by utilizing the Fourier transform a time trace can be translated

to the frequency domain. Different physical phenomena give rise to distinctively different frequency dependencies of the noise. The most widely understood is the thermal or shot noise, which has a flat or ‘white’ spectrum. In addition to this there is frequency dependent noise spectrum termed $1/f$ noise due to the inverse dependency of the noise power on the frequency. $1/f$ noise is ubiquitous in protein pore based sensors and the presence of increased $1/f$ often indicates increased membrane-protein interaction.

To gain further insight into the mechanism of this noise, the noise spectral densities, $S(f)$, of the data were computed. Experimental data was divided into 1 second windows and $S(f)$ was computed for each segment separately and subsequently averaged over the total number of segments. $S(f)$ of the current trace post-insertion are shown for both α -hemolysin and MspA in Fig. 2. The noise power spectral density for MspA exhibits a $1/f^2$ characteristic not seen in the α -hemolysin noise power spectrum.

Increased protein-polymer interaction can lead to multiple conformational interconversions with exponentially distributed time constants, the sum of which leads to $1/f^2$ like noise characteristics.¹⁷

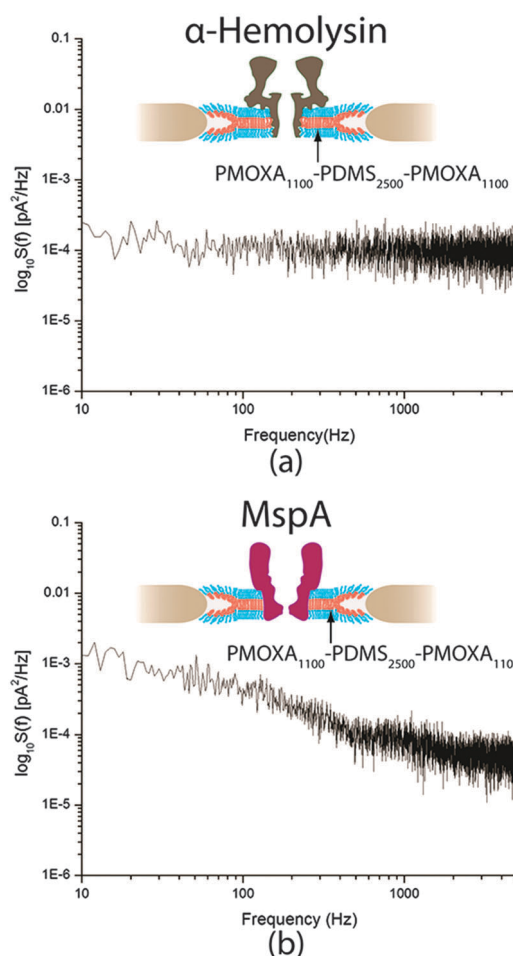


Fig. 2 Noise power spectral density of (a) α -hemolysin (b) MspA both in ABA1125. The spectrum of α -hemolysin has been scaled to account for capacitance differences.

Thus, the increase of $1/f^\alpha$ like noise characteristics (*i.e.* the increase in α) can be a viable indicator of increased protein-polymer interaction.

Contributions of substates to noise

Before comparing the noise properties of various polymer compositions or proteins it was important to examine the general origin of $1/f^\alpha$ behaviour. It has been previously observed that substate behaviour was the source of $1/f^\alpha$ characteristic seen in an open maltoporin channel's $S(f)$.¹¹

By excising sections of the time trace exhibiting substate behaviour, it was shown that the $1/f^\alpha$ noise was greatly reduced. This analysis was carried out on an ABA1125 (MspA insertion) time trace which showed sudden small dips in conductance, activity that is generally associated with the appearance of protein substates. Following this method utilized by Bezrukov and Winterhalter¹¹ we examined the effect of these substates on the noise power spectral density. The data was first lowpass filtered at 1 kHz with an 8-pole Butterworth filter; it was then smoothed with a 100 Hz moving average filter. A Gaussian distribution was fit to the histogram of the smoothed current trace data to define the major conduction state. The data points below the major conduction state identified through the earlier described process were eliminated from the raw data to produce a current trace without substates. Fig. 3 (bottom) shows the resultant $S(f)$ for both conductance traces before and after excision of substates.

Polymer composition and protein-membrane interactions

One possible reason for the increased substate activity is that the polar/nonpolar zones of MspA, unlike α -hemolysin, are not clearly defined¹⁸ leading to unfavourable membrane-protein interactions. Thus, the optimal membrane thickness needs to be determined experimentally. Block copolymers present two interrelated tuning parameters, the hydrophobic block length and the hydrophobic-hydrophilic ratio (f -ratio). As a starting point, the thickness of the hydrophobic B block was calculated using a method pioneered by Discher *et al.*¹⁶ This has been used for similar polymers in polymersome studies.¹⁹ In their work, it was found that the hydrophobic thickness (d) in nm of a similar polymer had a dependence on the molecular weight of the hydrophobic block (MW_{phob}) in kDa, corresponding to $d = \Phi(MW_{\text{phob}})^\zeta$ where Φ is a constant and ζ is a scaling factor equal to 0.5. Using this equation hydrophobic molecular weights of 2.5 and 3.5 kDa result in hydrophobic thickness values of 5.0 and 5.9 nm, respectively. These length values correspond well with the hydrophobic regions of α -hemolysin and MspA.^{18,20}

We first studied the effect of increasing hydrophobic thickness, while maintaining the molecular weight of the hydrophilic blocks. The increased block length was determined by choosing an f -ratio resulting in a slightly negative membrane curvature¹⁹ (PMOXA₁₁₀₀-PDMS₃₅₀₀-PMOXA₁₁₀₀) (ABA1135, Scheme 1). We then studied the effect of varying the f -ratio while keeping the hydrophobic thickness determined previously by reducing the molecular weight of the hydrophilic block (PMOXA₉₀₀-PDMS₃₅₀₀-PMOXA₉₀₀) (ABA935, Scheme 1) resulting in almost zero curvature.

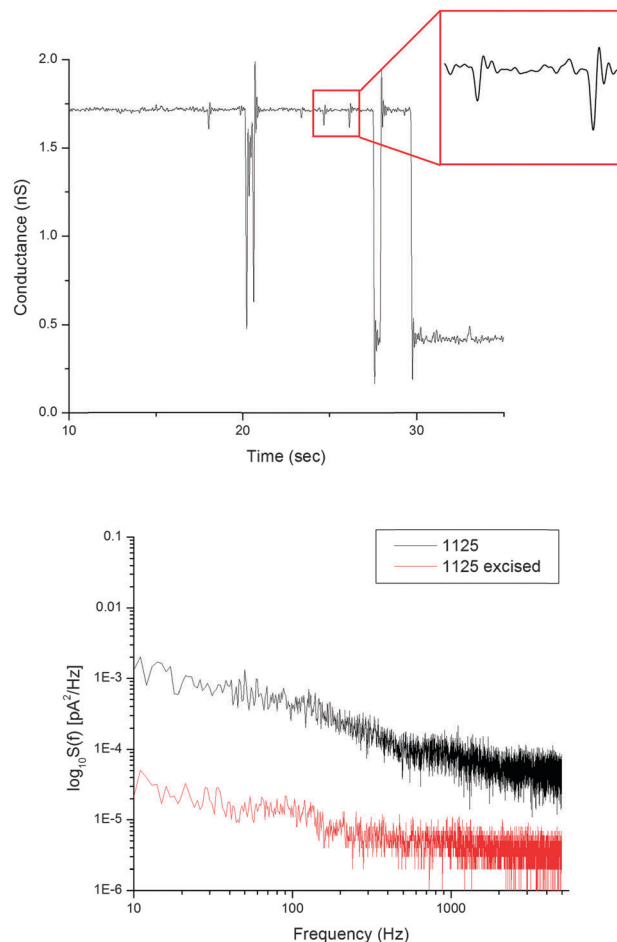


Fig. 3 (top) Conductance trace of a single insertion of MspA into 1125 with substate behaviour (inset). (bottom) Spectral density graphs of 1125 with (black, $\alpha = 0.7$) and without (red, $\alpha = 0.3$) substates incorporated into the trace.

MspA behaviour in different copolymer membranes

We tested three ABA copolymer membranes: ABA1135, ABA1125 and ABA935; all three were capable of MspA protein insertion (Fig. 4). Single protein insertion events were recorded for all three copolymer membranes typically upon addition of 1 μL of a 1 $\mu\text{g mL}^{-1}$ protein solution. At higher protein concentrations multiple insertion events were observed similar to the DPhPC lipid membrane. All analyses were performed using single protein insertion traces, since multiple insertions tend to provide more ambiguous data.

Examples of the resulting conductance traces are shown in Fig. 4. The average conductance values ($N = 8+$) of the protein's open state for the polymers were: ABA1135: 1.84 ± 0.24 nS, ABA1125: 1.62 ± 0.23 nS, and ABA935: 1.56 ± 0.29 nS. All were in close agreement with the average value of 1.60 nS reported for MspA in a lipid membrane.³ The similar conductance values suggest that the MspA pore retains its configuration in each membrane tested.

The background noise present in a protein pore embedded in a membrane effectively sets the limit of detection in protein pore based biosensors. From visual analysis of Fig. 4 it is evident the differences in current noise are considerable. The root

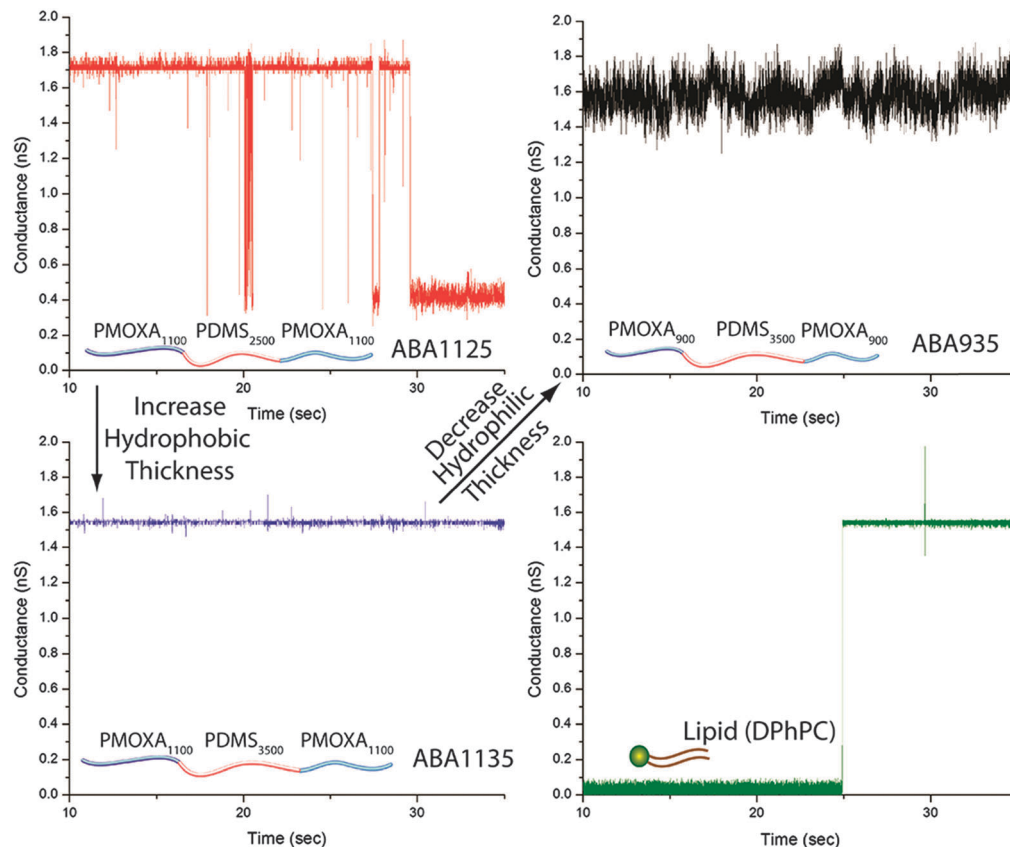


Fig. 4 Conductance traces over 20 seconds with an applied voltage of 60 mV for a single MspA insertion into ABA1125 (top left), ABA1135 (bottom left), ABA935 (top right) and DPhPC (lipid) (bottom right). All traces filtered with 10th-order Butterworth filter at 100 Hz.

mean squared (rms) current value for each trace provides more information into the magnitude of noise for a specified bandwidth for each protein–membrane system. For MspA in lipid, the rms value for a bandwidth of 1 kHz of a single insertion was found to be $0.35 \text{ pA}_{\text{rms}}$. The average rms values ($N = 8+$) for the polymers were calculated to be $2.91 \pm 1.44 \text{ pA}_{\text{rms}}$ (ABA935), $1.01 \pm 0.5 \text{ pA}_{\text{rms}}$ (ABA1135), and $4.12 \pm 4.30 \text{ pA}_{\text{rms}}$ (ABA1125). It seems both f -ratio and hydrophobic mismatch are capable of modulating the resulting noise profile of an inserted MspA protein. As mentioned previously, noise effects are dependent on subtle protein–membrane interactions, some of which can be scrutinized using spectral analysis.²¹

$S(f)$ was computed for each protein's open state when minimal gating was present. Spectra of the membranes before and after a single protein insertion are shown in Fig. 5. Prior to insertion, $S(f)$ for all membranes were nearly identical. However, post-insertion the membrane spectra displayed considerably different behaviours. $S(f)$ for the traces in Fig. 5 show ABA935 and the ABA1125 displayed $1/f^\alpha$ behaviour with $\alpha \approx 0.98$ and $\alpha \approx 0.70$, respectively. The DPhPC exhibited a white spectrum, the ABA1135 spectrum was near white ($\alpha \approx 0.20$) and close to the noise floor of the amplifier.

The correlation of the noise power spectrum and the increased noise in the time traces of conductance (see Fig. 4) show the increase in the current noise was mainly due to an increase in flicker noise of the pore. Some variation in $1/f^\alpha$ behaviour was

observed between different trials in each polymer, which may stem from polydispersity effects causing polymer membranes to be less uniform than their lipid counterparts. This is particularly true for PDMS containing polymers synthesized using cationic ring-opening polymerization yielding a polydispersity index close to 2.²² Thus, a single protein could feasibly insert into different pockets of polymer length, leading to changes in the noise profile. This effect is currently under investigation in the lab.

The change in $S(f)$ post-insertion strongly suggests the increase in noise is due to membrane–protein interactions^{21,23,24} and is not an intrinsic property of the membrane. One possible reason for this increased interaction may be the random insertion of the hydrophilic polymer segment into the pore. This can be ruled out because a triblock polymer (ABA1135) with the same hydrophobic block as ABA935 and longer hydrophilic block exhibited no $1/f^\alpha$ noise behaviour. Furthermore, a polymer with the same hydrophilic thickness but reduced hydrophobic thickness (ABA1125) exhibited lower $1/f^\alpha$ behaviour. Hydrophobic mismatch can give rise to lateral and compressive strain in the membrane and translates to changes in the energy barriers between different protein conformational states.²⁵ This can affect the protein's behaviour by exposing or hiding different substates. The rim domain of MspA being partially buried in the membrane due to exposed hydrophobic residues coupled with its conical shape could exacerbate this effect.¹⁸ Another possibility could be that click-coupling based synthesis results in incomplete

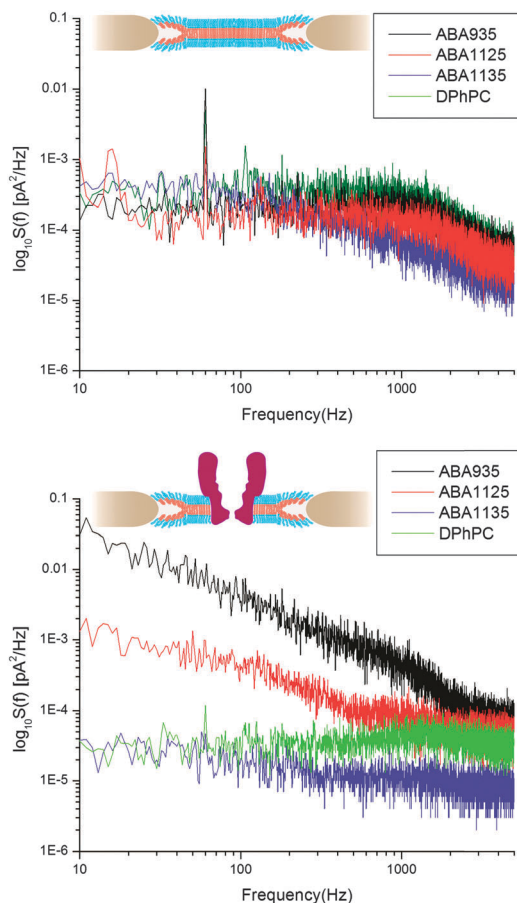


Fig. 5 Noise power spectral density of a single MspA inserted into polymer and lipid membranes. The top plot examines the noise properties of the membranes prior to protein insertion, while the bottom shows post-insertion data. Spectra are taken of the single traces shown in Fig. 4 to clearly illustrate noise profiles of those traces. The $1/f^2$ behaviour of the power spectral density clearly arises solely from the membrane–protein interactions and is not an intrinsic property of the membrane.

conjugation resulting in a mixture of tri and diblocks thereby increasing the noise. This can be ruled out for two reasons, one the noise only occurs in MspA but not in hemolysin and the polymer membranes intrinsically do not show this noise behaviour. More importantly, we also studied the insertion of MspA in a commercially available ABA PMOXA₅₅₀–PDMS₂₆₀₀–PMOXA₅₅₀ (Polymer Source) synthesized using an alternative method (macroinitiation), which also exhibited the same increased noise and gating behaviour similar to ABA935 and ABA1125 (see ESI,† Fig. S9 and S10). These results indicate the most plausible reason for the increased noise is the increased membrane–protein interaction due to hydrophobic mismatch and membrane curvature. Hence, it is crucial the ABA polymer membrane be tailored to reduce the deleterious effects of this interaction.

Conclusions

We present for the first time experimental evidence of polymer membrane composition on the substates exhibited by an MspA nanopore. Unlike previous studies, by utilizing a modular

synthetic approach, we methodically varied the f -ratio and studied its effect on the noise properties of the protein. Although polymer membranes are known to be more tolerant of hydrophobic mismatch, there is enough membrane–protein interaction to give rise to drastically different noise properties between different proteins (*i.e.* MspA versus α -hemolysin). This necessitates careful optimization of polymer membranes to provide superior biosensors. Work is ongoing in our lab in designing single molecule biosensors using protein nanopores embedded in polymer membranes.

Acknowledgements

This work was supported by the National Institutes of Health, through the NIH Director's New Innovator Award Program (1-DP2-OD007472-01), National Human Genome Research Institutes (NHGRI) \$1000 Genome Program Grant R01HG005115 and the National Science Foundation under Award No. DMR-1121053.

Notes and references

- 1 D. Branton, D. W. Deamer, A. Marziali, H. Bayley, S. A. Benner, T. Butler, M. Di Ventra, S. Garaj, A. Hibbs, X. H. Huang, S. B. Jovanovich, P. S. Krstic, S. Lindsay, X. S. S. Ling, C. H. Mastrangelo, A. Meller, J. S. Oliver, Y. V. Pershin, J. M. Ramsey, R. Riehn, G. V. Soni, V. Tabard-Cossa, M. Wanunu, M. Wiggin and J. A. Schloss, *Nat. Biotechnol.*, 2008, **26**, 1146–1153.
- 2 I. M. Derrington, T. Z. Butler, M. D. Collins, E. Manrao, M. Pavlenok, M. Niederweis and J. H. Gundlach, *Proc. Natl. Acad. Sci. U. S. A.*, 2010, **107**, 16060–16065.
- 3 T. Z. Butler, M. Pavlenok, I. M. Derrington, M. Niederweis and J. H. Gundlach, *Proc. Natl. Acad. Sci. U. S. A.*, 2008, **105**, 20647–20652.
- 4 M. Winterhalter, *Curr. Opin. Colloid Interface Sci.*, 2000, **5**, 250–255.
- 5 E. T. Castellana and P. S. Cremer, *Surf. Sci. Rep.*, 2006, **61**, 429–444.
- 6 A. Gonzalez-Perez, K. B. Stibius, T. Vissing, C. H. Nielsen and O. G. Mouritsen, *Langmuir*, 2009, **25**, 10447–10450.
- 7 M. J. Isaacman, K. A. Barron and L. S. Theogarajan, *J. Polym. Sci., Part A: Polym. Chem.*, 2012, **50**, 2319–2329.
- 8 C. Nardin, M. Winterhalter and W. Meier, *Langmuir*, 2000, **16**, 7708–7712.
- 9 W. Meier, A. Graff, A. Diederich and M. Winterhalter, *Phys. Chem. Chem. Phys.*, 2000, **2**, 4559–4562.
- 10 E. A. Manrao, I. M. Derrington, A. H. Laszlo, K. W. Langford, M. K. Hopper, N. Gillgren, M. Pavlenok, M. Niederweis and J. H. Gundlach, *Nat. Biotechnol.*, 2012, **30**, 349–353.
- 11 S. M. Bezrukov and M. Winterhalter, *Phys. Rev. Lett.*, 2000, **85**, 202–205.
- 12 N. N. Jetha, M. Wiggin and A. Marziali, *Methods Mol. Biol.*, 2009, **544**, 113–127.
- 13 P. Kramar, D. Miklavcic and A. M. Lebar, *Bioelectrochemistry*, 2007, **70**, 23–27.
- 14 W. Meier, C. Nardin and M. Winterhalter, *Angew. Chem., Int. Ed.*, 2000, **39**, 4599–4602.

- 15 G. Srinivas, D. E. Discher and M. L. Klein, *Nano Lett.*, 2005, **5**, 2343–2349.
- 16 G. Srinivas, D. E. Discher and M. L. Klein, *Nat. Mater.*, 2004, **3**, 638–644.
- 17 R. Sauve and G. Szabo, *J. Theor. Biol.*, 1985, **113**, 501–516.
- 18 M. Mahfoud, S. Sukumaran, P. Hulsmann, K. Grieger and M. Niederweis, *J. Biol. Chem.*, 2006, **281**, 5908–5915.
- 19 D. E. Discher and A. Eisenberg, *Science*, 2002, **297**, 967–973.
- 20 L. Song, M. R. Hobaugh, C. Shustak, S. Cheley, H. Bayley and J. E. Gouaux, *Science*, 1996, **274**, 1859–1866.
- 21 Z. Siwy and A. Fulinski, *Phys. Rev. Lett.*, 2002, **89**, 158101.
- 22 H. A. Klok, P. Eibeck, M. Moller and D. N. Reinhoudt, *Macromolecules*, 1997, **30**, 795–802.
- 23 E. Perozo, D. M. Cortes, P. Sompornpisut, A. Kloda and B. Martinac, *Nature*, 2002, **418**, 942–948.
- 24 N. Mobashery, C. Nielsen and O. S. Andersen, *FEBS Lett.*, 1997, **412**, 15–20.
- 25 O. S. Andersen and R. E. Koeppe, 2nd, *Annu. Rev. Biophys. Biomol. Struct.*, 2007, **36**, 107–130.